PhD Project Report

STRUCTURAL HISTORY OF TASMANIA FROM THE DEVONIAN – RECENT

Introduction

The main aim of this project is to establish the geometry and timing of structures affecting all the sedimentary sequences in and underlying the Tasmania Basin from the early Palaeozoic through to the Tertiary. The exact timing of folding and faulting in the Tasmania Basin is critical in the assessment of the Gondwana Petroleum System and its relationship to hydrocarbon maturation, migration and trap formation. The geometry of folds and faults within the Lower-Middle Palaeozoic's is critical to understanding the Larapintine Petroleum System.

This study will provide structural input into the ARC SPIRT project: *Petroleum Systems Modelling Onshore Tasmania.* The structural history, especially the definition of hydrocarbon traps, migration fairways, palinspastic restorations of source kitchens and uplift and thermal history will be integrated into a three dimensional model of onshore petroleum systems in Tasmania, this work performed in close association with other project team members.

Seismic Data

Introduction

In March 2001 GSLM acquired 659 line kilometres of seismic reflection data across the Central Highlands and in the Northern Midlands areas (Tasmanian Basin Seismic Survey TB-O1)(Figure 1). The data was acquired for GSLM by Trace Terracorp using the vibroseis method and “crooked line” type grid (shot mainly along roads), processing of the data is by Robertson Research and the subsequent interpretations have been made utilising The Kingdom Suite™ seismic interpretation software.

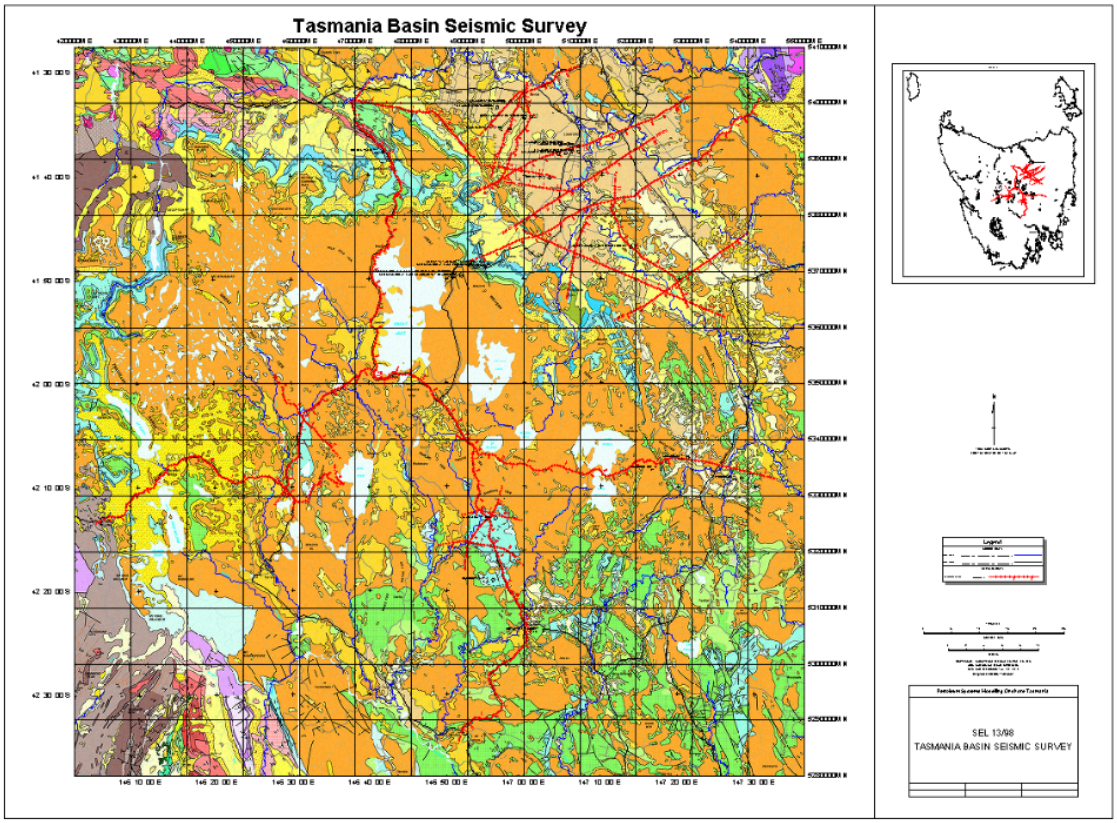

Figure 1: Tasmania Basin Seismic Survey (TB-01) line location map.

Seismic Data Quality

The quality of the seismic data set is highly variable, individual sections contain zones of strongly coherent events as well as zones of noise; consequently coherent events across sections are rare. The variability in the data are likely to result from the "crooked-line" grid employed during acquisition, outcropping dolerite and from the velocity picks applied during processing.

The use a "crooked line" grid (shooting along existing roads) and the vibroseis method has enabled GSLM to acquire an extensive regional data set whilst minimising the expense. However seismic data acquired along straight lines is more easily ascribed to geologic rather then acquisition changes. Processing techniques generally assume a straight line profile with uniform fold and even offsets, crooked line acquisition results in variable fold and uneven offsets (Wu 1996). Specialised processing with careful initial and residual statics corrections and frequent velocity analysis are required, and even with crooked line processing methods applied, problems such as seismic transparent zones and coherent noise can still result where there are changes in survey line direction (Wu 1996).

Dolerite has been a major deterrent to petroleum exploration in Tasmania, with nearly every part of the basin being intruded by at least one dolerite sill. The seismic data acquired across the Central Plateau and the Longford Sub-basin, demonstrates the variations in data quality associated with shooting seismic through the dolerite. When at, or near, the surface, dolerite is generally highly diffusive resulting in poor resolution of underlying events (Fig 2, 1800-2200). Whether this results from the effects of weathering, or the occurrence of boulders or remnant boulder fields in the soil profile is unclear. At depth, the dolerite is characterised by a

strong positive event at its top and base and by weak and scattered events in between. Seismic events beneath the dolerite are in general, better resolved (Fig 2, 2250-2350).

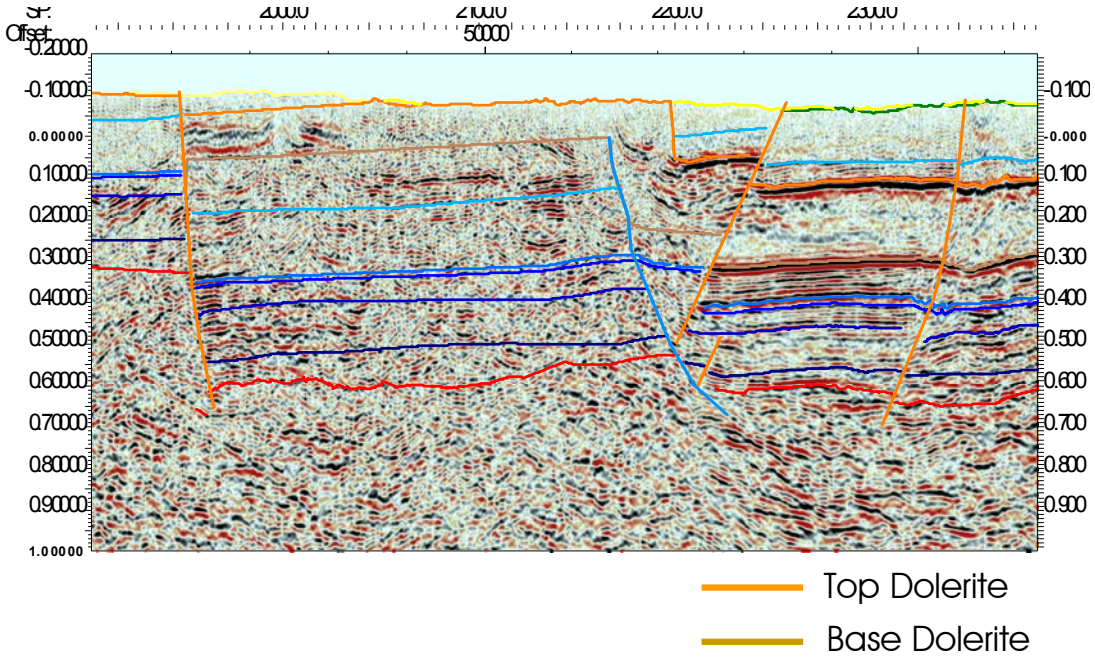

Figure 2: Variations in seismic resolution due to dolerite – line TB01-ST.

Geologic Controls on Seismic Data

The control provided by wells, on seismic data is essential in relating seismic events to stratigraphy. There are very few deep wells i.e. wells that sample rocks from below the Parmeener Supergroup in the survey area and those that are available are not always on or close enough to a seismic line to be useful (Figure 1).

There are 2 methods used to tie geology to seismic data:

1) Using a time depth function calculated from checkshot data, or
2) Tying to the seismic data using a synthetic seismogram (Tearpock & Bische 2003).

Synthetic seismograms are the preferred method as they provide the best results, their generation requires the combination of sonic and density data logs and checkshot surveys from wells. Unfortunately there are no drillholes in the survey area that have had these logs recorded and therefore tying seismic data to well data cannot be achieved using this method.

A simple but less accurate method is to conduct a checkshot survey and use the measured velocities to convert formation tops in the drillholes from depth to time, which can then be plotted on to a seismic section. The only checkshot survey conducted in Tasmania (to my knowledge) was on Bruny Island in the Shittim #1 drillhole. Patrick Fournier performed the survey where he measured the velocity of the dolerite found in the hole and the temperature gradient as part an honours thesis at the University of Tasmania (Fournier 2000).

Hunterston #1 DDH Velocity Survey

Aim

The aim of the velocity survey was to use a downhole sonde (Fournier 2000) to acquire velocity data at multiple levels in the Hunterston #1 DDH. The data was acquired at or as near as possible to formation boundaries (identified from core), therefore the resultant data represents the velocities across those formations. This data will then be used to as a means to convert between depth and time, enabling the formation boundaries to be plotted in time, onto seismic sections acquired adjacent to the Hunterston #1 DDH. Velocity data can also be applied to other drillholes with the same stratigraphy enabling formation boundaries to be plotted onto other seismic sections in the Tasmania Basin Seismic Survey. The accurate positioning of these formation boundaries on the seismic sections will greatly improve the accuracy of the interpretation.

Equipment

The system used to conduct the survey was developed by Patrick Fournier as part of an Honours thesis at the University of Tasmania (Fournier 2000). The system consists of two main elements; a sonde containing a temperature sensor, a geophone, their associated electronics and a power supply (Figure 3) and a flat top trailer on which rides 1000m of communication cable labelled every 25 metres starting at the tail of the sonde and attached to a 12 VDC winch, 1000m of strength cable running through a counter (Figure 4). Seismic energy was provided by Powergel using zero delay detonators, the seismic data was recorded with a Geometrics ES-1225 seismograph the records then downloaded onto a laptop computer using *Seisview*™ seismic refraction interpretation software.

Figure 3: Sonde for measuring downhole velocity and temperature.

Figure 4: Trailer rig and seismic recorder for sonde.

Procedure

Data Acquisition:

Cracking the drill rods at the collar allowed the sonde to be lowered through the rods into the open well. The trailer with the communications and strength cable was positioned adjacent to the well, the cables running via a set of pulleys slung from the derrick, guiding the cables into the well. The energy source was fired 50m from and 6m below the well collar in a pond, which provided good coupling between the seismic energy source and the ground.

The sonde was lowered into the well, the distance below the collar calculated to the nearest metre by using the labels on the cable in concert with the counter on the strength cable. When the desired depth was reached, the cables were clamped at the top of the well and the tension between the well collar and cable reels released to reduce the any noise induced by the cables.

The seismograph would then be connected to the communications cable (this connection could not be maintained when the cable reel was moving during raising or lowering); the charge would then be readied for the shot. When the shot was fired a signal would be generated to trigger the seismograph. On completion of the shot, the seismograph would be checked to ensure the data was recorded successfully, the data downloaded onto a laptop computer and the seismograph cleared and readied for the next shot. The cable connecting the seismograph to the communications cable would then be removed, the clamps at the collar removed and the sonde lowered to the position of the next shot, the above process then repeated for the next shot.

Shots were taken at varying intervals in the well to best ascertain the velocities across and within the formations identified in the Hunterston #1 DDH (Figure 5). Nine shots were taken in all, shot 1 was taken to ascertain the velocity of the weathering layer, shot 2 for the velocity in the Ferntree Mudstone, shots 3-6 to ascertain the variation in velocity variation in the Jurassic Dolerite, shot 7, 8 and 9 to ascertain the velocity of the Cascades Group, the Liffey Group and the Bundella correlate respectively.

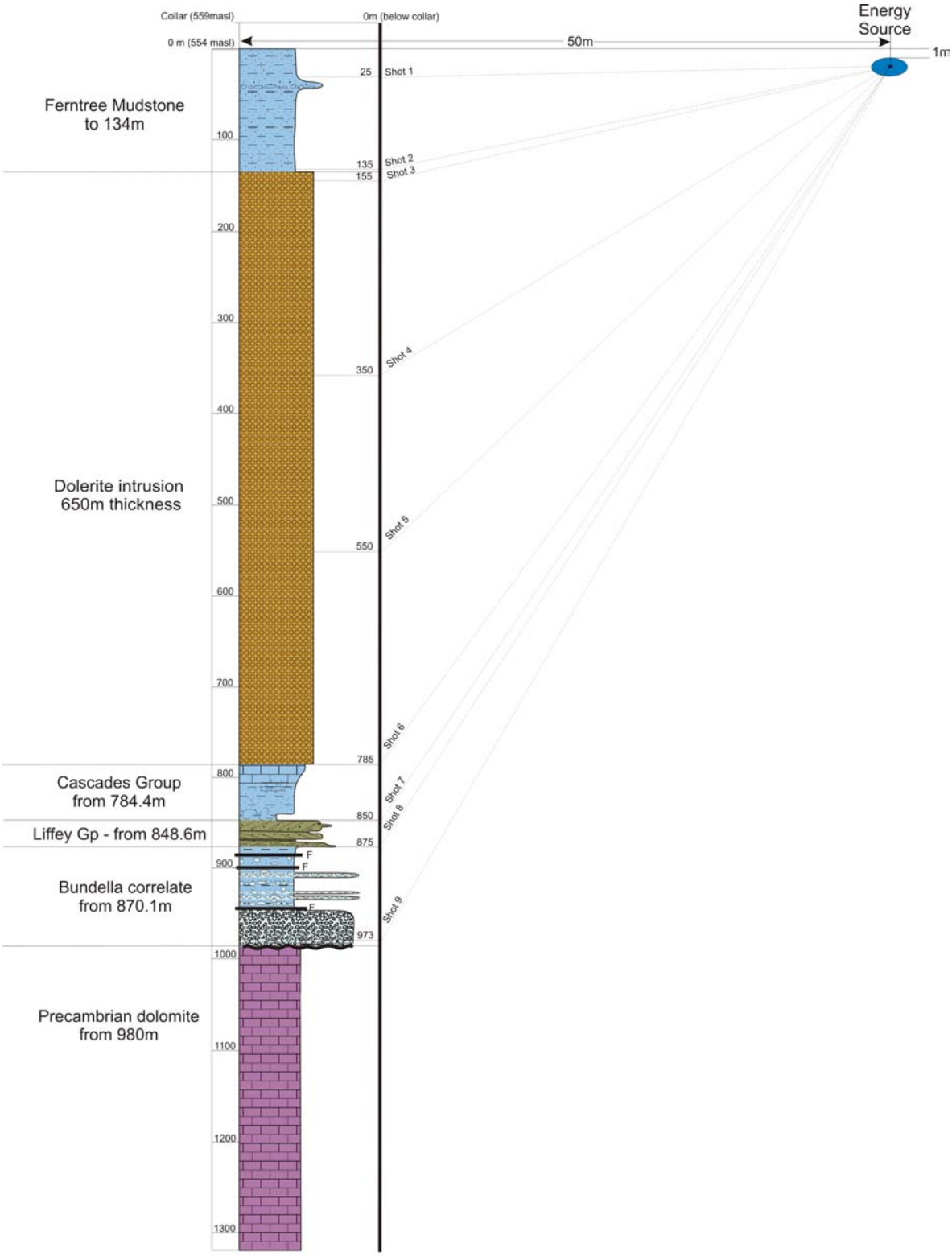

Figure 5: Hunterston #1 DDH velocity survey shots and raypaths.

Interpretation:

The data recorded by the seismograph and downloaded onto the laptop computer were the seismic energy arrival times at the geophone in the sonde (one-way times)(Figure 6). The initial arrivals of seismic energy or first breaks are the times required to calculate velocity. The first breaks for this data set are troughs; the times were picked as the first negative deflection of the signal into the first large trough of the seismic record (Figure 6).

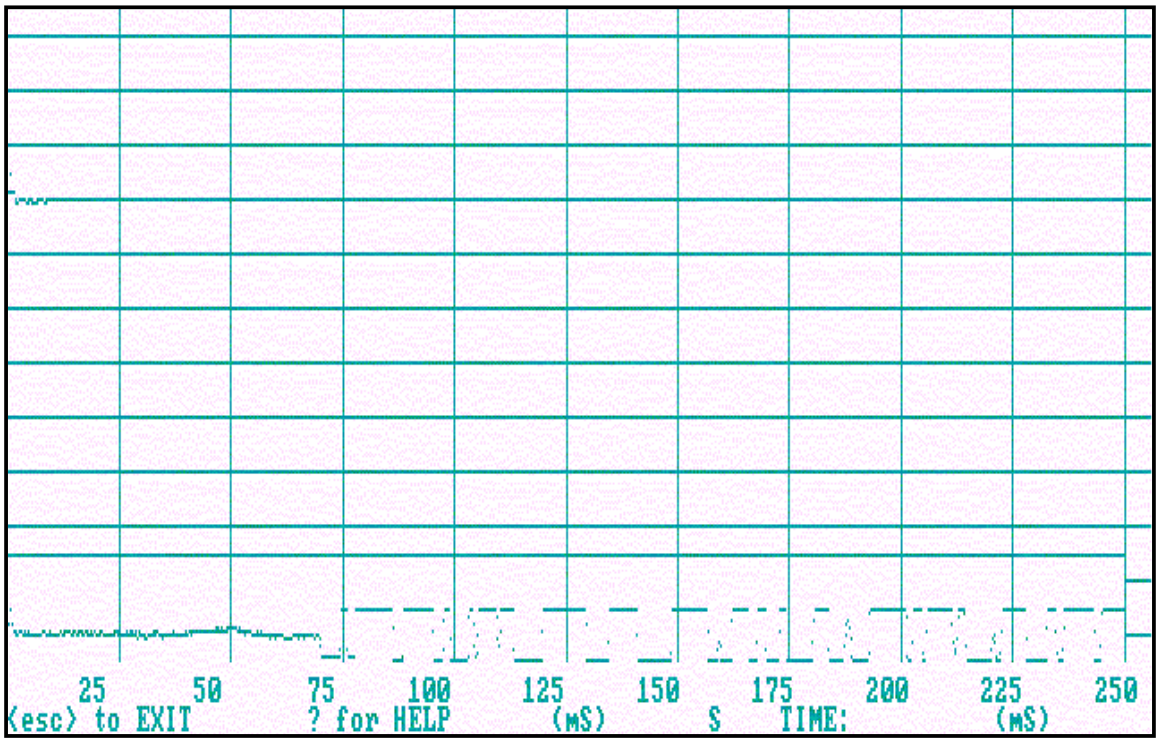

Figure 6: Seismic data record with first break for shot at 350m (below collar).

Once the first brakes were picked and recorded the cumulative and interval velocities could be calculated using the equation (Table 1):

Hunterston #1 DDH - Velocity Survey											
Collar Height: 5m Distance Collar-Source: 50m Elevation difference well-source: -1m											
Shot	Filename	Depth from Collar (m)	Depth below ground level (m) (referenced to source)	Distance shot-geophone (m)	1-way time (sec)	2-way time (sec)	Shot-geophone cumulative velocity	Distance difference (cumulative)	Time difference (cumulative)	Interval	Interval Velocity
1	hunt25d	25	19	53.48832	0.01700	0.03400	3146.37176	0.00000	0.00000	0-25 Weathered Layer	3146.37
2	hunt135a	135	129	138.35100	0.03525	0.07050	3924.85115	20.37728	0.00648	25-135 Ferntree Mudstone	4100.07
3	hunt155a	155	149	157.16552	0.03875	0.07750	4055.88433	136.06948	0.03467	135-155 Top Dolerite	5168.95
4	hunt350a	350	344	347.61473	0.06975	0.13950	4983.72372	150.56522	0.03712	155-350 Intra-Dolerite 1	6039.42
5	hunt550a	550	544	546.29296	0.09725	0.19450	5617.40835	345.44996	0.06932	350-550 Intra-Dolerite 2	7189.82
6	hunt785a	785	779	780.60297	0.13300	0.26600	5869.19528	545.11941	0.09704	550-785 Base Dolerite	6548.68
7	hunt850b	850	844	845.47975	0.14550	0.29100	5810.85736	780.36578	0.13296	785-850 Cascades Gp	5192.33
8	hunt875a	875	869	870.43725	0.15150	0.30300	5745.46037	845.39590	0.14549	850-875 Liffey Gp	4163.55
9	hunt973a	973	967	968.29179	0.17400	0.34800	5564.89537	870.16088	0.15145	875-973 Bundella	4352.07

Table 1: Results of the Hunterston #1 DDH velocity survey.

$v=d/t$ v = velocity (m/s), d = distance (m) and t = time (seconds) {eqn. 1}

To calculate the interval velocity, the time and distance difference between an interval and all its preceding intervals had to be calculated so that only the time taken and the distance travelled through that particular interval were considered by the equation (Table 2).

Interval Velocity Calculations - Hunterston #1 DDH													
Interval 0-25m (Weathered Layer)													
Hole-source distance	Depth (m) (referenced to source elevation)	Source-geophone distance	1-way time (sec)	Angle 'a' (Degrees)	D_1	Velocity (D_1) (Interval Velocity)							
50	19	53.48831648	0.01700	69.19320899	53.48831648	3146.371558							
Interval 25-135 (Ferntree Mudstone)													
Hole-source distance	Depth (m) (referenced to source elevation)	Source-geophone distance	1-way time (sec)	Angle 'a' (Degrees)	D_1	D_2	Time Difference ($t_1=d_1/v$)	Velocity (D_2) (Interval Velocity)					
50	129	138.3510029	0.03525	21.18617644	20.3772795	117.9737234	0.006476438	4100.073613					
Interval 135-155 (Top Dolerite)													
Hole-source distance	Depth (m) (referenced to source elevation)	Source-geophone distance	1-way time (sec)	Angle 'a' (Degrees)	D_1	D_2	D_3	Time Difference ($t_1=d_1/v$)	Time Difference ($t_2=d_2/v$)	Total Time Difference	Velocity (D_3) (Interval Velocity)		
50	149	157.1655178	0.03875	18.55023193	20.04124053	116.0282347	21.09604266	0.006369636	0.028299061	0.034668697	5168.947936		
Interval 155-350 (Intra Dolerite-1)													
Hole-source distance	Depth (m) (referenced to source elevation)	Source-geophone distance	1-way time (sec)	Angle 'a' (Degrees)	D_1	D_2	D_3	D_4	Time Difference ($t_1=d_1/v$)	Time Difference ($t_2=d_2/v$)	Time Difference ($t_3=d_3/v$)	Total Time Difference	Velocity (D_4) (Interval Velocity)
50	344	347.6147293	0.06975	8.269961587	19.19965074	111.1558727	20.21015868	197.0490471	0.006102156	0.027110702	0.003909917	0.037122775	6039.405684
Interval 350-550 (Intra Dolerite-2)													
Hole-source distance	Depth (m) (referenced to source elevation)	Source-geophone distance	1-way time (sec)	Angle 'a' (Degrees)	D_1	D_2	D_3	D_4	D_5	Time Difference ($t_1=d_1/v$)	Time Difference ($t_2=d_2/v$)	Time Difference ($t_3=d_3/v$)	Time Difference ($t_4=d_4/v$)
50	544	546.2929617	0.09725	5.251401822	19.08008506	110.4636503	20.08430006	195.8219256	200.8430006	0.006064155	0.02694187	0.003885568	0.032424039
Interval 550-785 (Base Dolerite)													
Hole-source distance	Depth (m) (referenced to source elevation)	Source-geophone distance	1-way time (sec)	Angle 'a' (Degrees)	D_1	D_2	D_3	D_4	D_5	D_6	Time Difference ($t_1=d_1/v$)	Time Difference ($t_2=d_2/v$)	Time Difference ($t_3=d_3/v$)
50	779	780.6029721	0.13300	3.672483507	19.03909688	110.2263504	20.04115461	195.4012574	200.4115461	235.4835667	0.006051128	0.026883993	0.003877221
Interval 785-850 (Cascades Group)													
Hole-source distance	Depth (m) (referenced to source elevation)	Source-geophone distance	1-way time (sec)	Angle 'a' (Degrees)	D_1	D_2	D_3	D_4	D_5	D_6	D_7	Time Difference ($t_1=d_1/v$)	Time Difference ($t_2=d_2/v$)
50	844	845.4797455	0.14550	3.39033722	19.03331181	110.1928578	20.03506506	195.3418843	200.3506506	235.4120144	65.11396144	0.006049289	0.026875824
Interval 850-875 (Liffey Group)													
Hole-source distance	Depth (m) (referenced to source elevation)	Source-geophone distance	1-way time (sec)	Angle 'a' (Degrees)	D_1	D_2	D_3	D_4	D_5	D_6	D_7	D_8	Time Difference ($t_1=d_1/v$)
50	869	870.4372464	0.15150	3.293019443	19.03142426	110.1819299	20.03307817	195.3225121	200.3307817	235.3886685	65.10750405	25.04134771	0.006048689
Interval 875-973 (Bundella Correlate)													
Hole-source distance	Depth (m) (referenced to source elevation)	Source-geophone distance	1-way time (sec)	Angle 'a' (Degrees)	D_1	D_2	D_3	D_4	D_5	D_6	D_7	D_8	D_9
50	967	968.2917949	0.17400	2.959917289	19.0253817	110.1469467	20.02671758	195.2604964	200.2671758	235.3139315	65.08683213	25.03339697	98.13091613

Table 2: Internal velocity calculations, Hunterston #1 DDH.

Results

The results of the velocity survey are displayed in tables 1 and 2. Two interesting features are observed in the data. Firstly, that there is a considerable variation in velocity within the Jurassic dolerite, this variation was explored by Fournier (2000) who found that coarse-grained dolerite was slower (≈ 6200 m/s) than finer grained varieties. Secondly, that the velocity of the Liffey Group was considerably lower then that of the surrounding strata, which should result in a strong event corresponding to the top of the Liffey Group on the seismic sections.

Seismic Data Interpretation

The interpretation of the data from the TB-01 Seismic Survey is an important part of the Structural History project. The interpretation process has been an iterative one, with improvements to the interpretation being continually made as data to constrain the interpretation is incorporated. Recent advances have resulted from control provided by the incorporation of well logs, well data and the results of the velocity survey.

All the survey lines have been interpreted, although some have been the subject of greater effort then others depending upon the overall data quality, availability of other data to constrain the interpretation and/or the needs of the current drilling program. The interpretation of the lines acquired over the Longford Sub-Basin is the subject of an honours thesis at the University of Tasmania (Lane 2002).

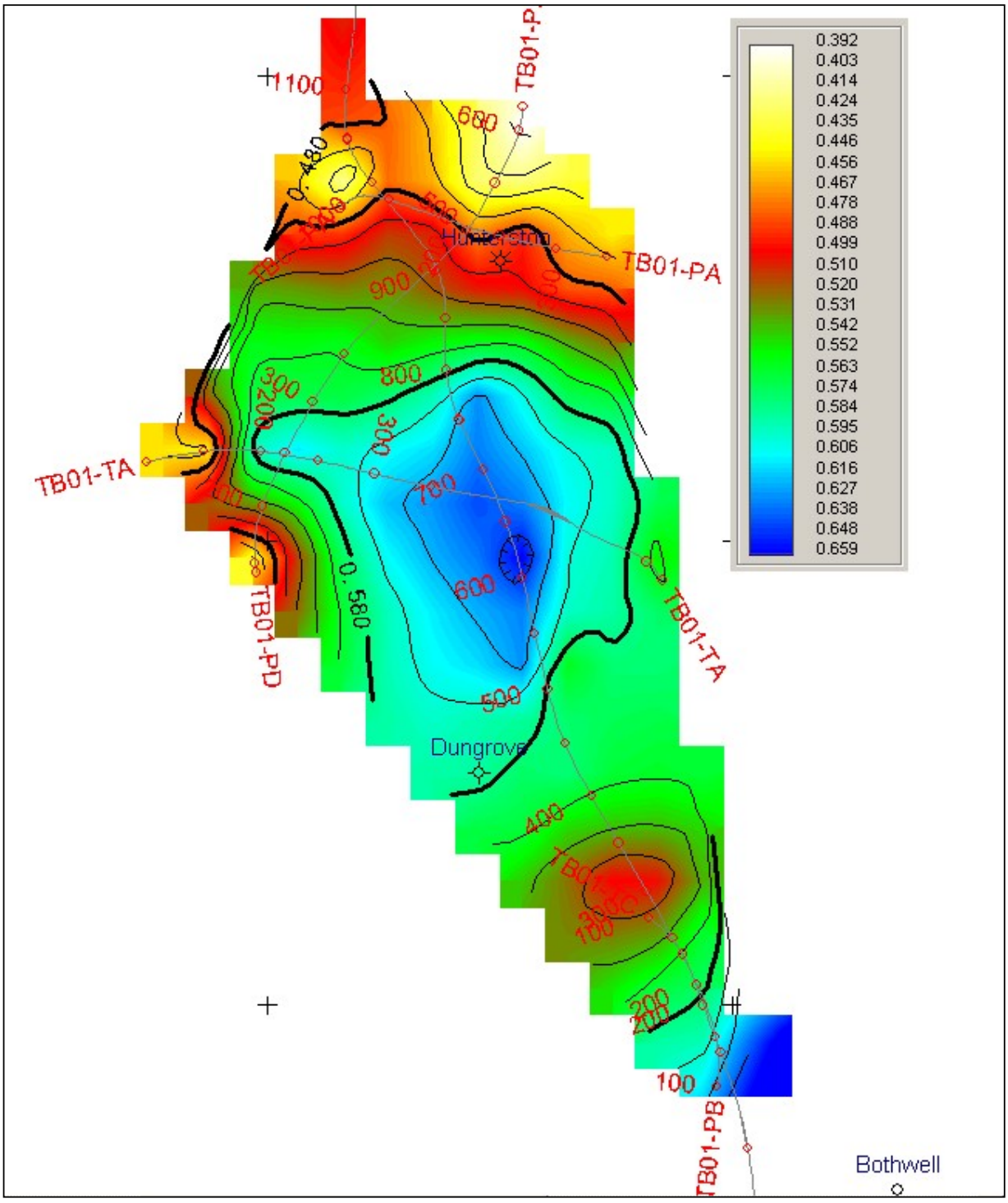

Figure 7: Two-way time structure map of the top dolerite horizon, Hunterston prospect.

The work on the Tasmania Basin sequences has generally been conducted where there are "windows" in the dolerite or where the resolution is good. The best examples are the Hunterston and Bronte/Bellevue prospects and the eastern end of line TB-01 ST.

Hunterston

The Hunterston prospect is at the northern end of one such window (490000 mE, 5320000 mN). Fairbridge (Fairbridge 1949) was the first to notice the gently dipping Permian strata of the area formed a domal structure (Hunterston Dome), which he thought had lost their dolerite capping and had been eroded out into physiographic basin because of their elevation. The Hunterston #1 DDH was pre-collared in August 1997 to a depth of 336 m intersecting dolerite at 134 m (Tanner & Burrett 1997). Fairbridge's interpretation was revised by GSLM geologists to include a second dolerite sill (Tanner & Burrett 1997). Interpretation of seismic lines TB-01 PA, PB, PD and TA with the control from the Hunterston #1 DDH has revealed that a single, bowl shaped dolerite sill underlies the Permian strata and that the Hunterston Dome has been created by a small, higher relief area on the northeastern edge of the intrusion (Figure 7).

Bronte/Bellevue

The Bronte/Bellevue prospect is located in another Permian window between the village of Bronte Park and the Bellevue Tier (460000mE, 5330000mN). Seismic lines TB-01 PB, and TD resolve events particularly well here, except in those areas where there are bends in the roads along which the data was acquired. Interpretation of the seismic data for the Permian section predicts a ~100m veneer of the upper glaciomarine sequence of the Parmeener

Supergroup followed by a ~800m thick dolerite sill with a further 400-450m of Permian rocks to the predicted Base Parmeener Unconformity (Figure 8).

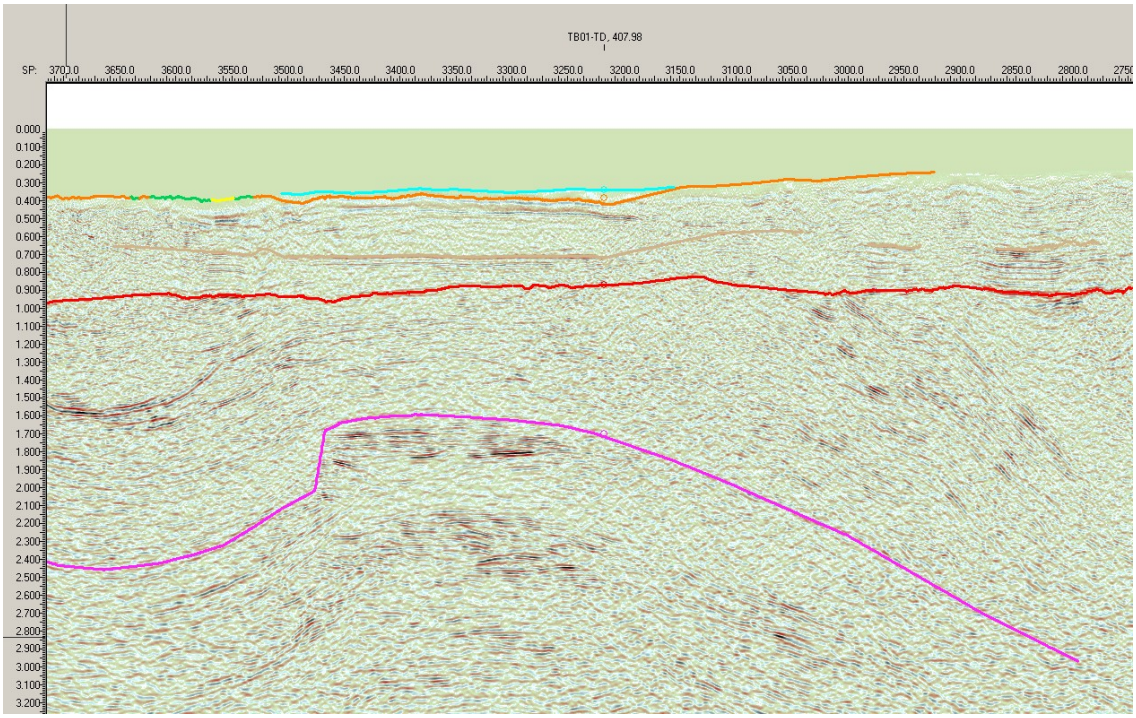

Figure 8: Interpretation of the Permian section, Bronte/Bellevue prospect.

Deeper structures are resolved by seismic lines TB-01 PB, TB, TD and TI, however it is unclear what rock units form these structures. The structure has been interpreted as northwesterly plunging antiform (Figure 9), the strike of which would appear to be a continuation of the northwesterly striking Deloraine/Railton trend (Williams et al. 1989).

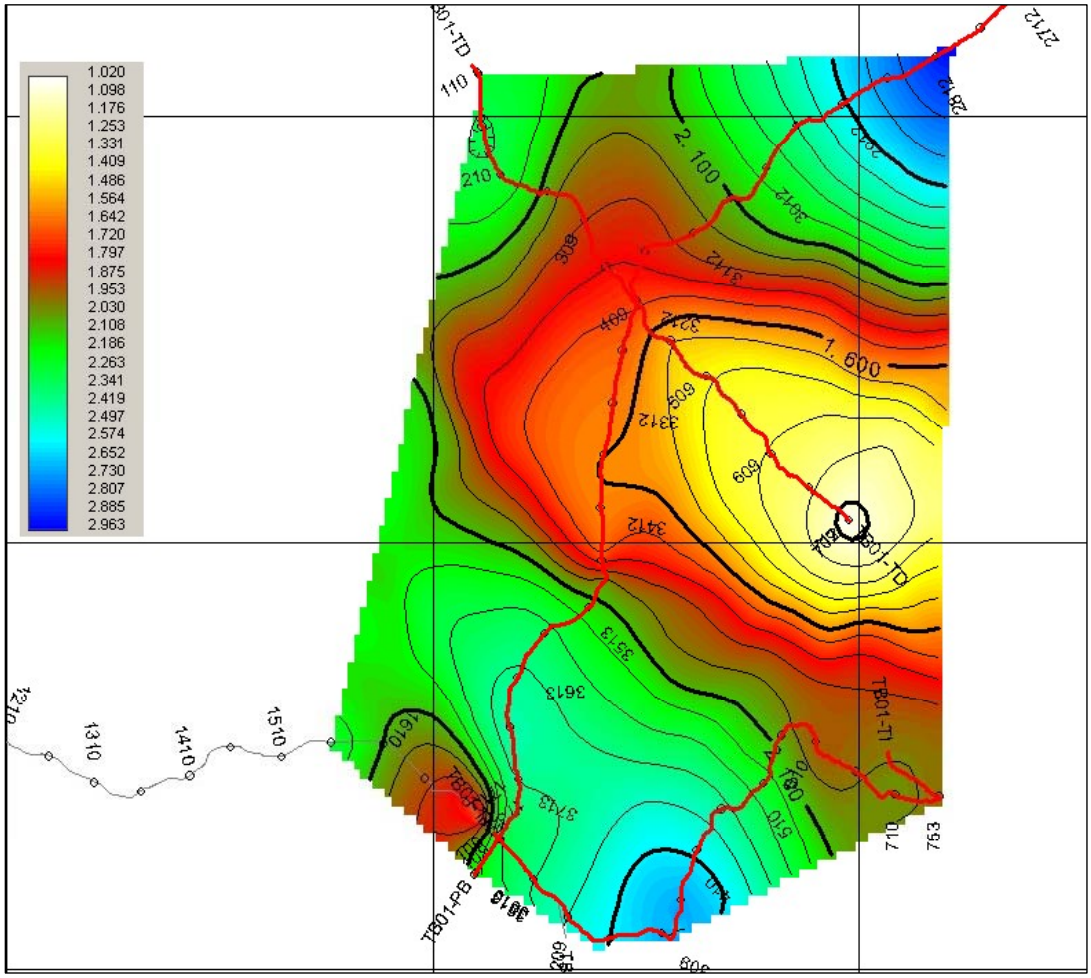

Figure 9: Two-way time structure map of the basement structure, Bronte/Bellevue prospect

Eastern end of Seismic Line TB-01 ST

The eastern end of line TB-01 ST is constrained by the deep drillholes Tunbridge RG145, Ross 1 (Quoin) and Ross RG146 (Ross 1) and by the shallower drillholes Annandale 1 and Woodbury 11 (Figure 1). The relatively flat lying Permian sequence is dissected by a complex

series of faults most of which appear to postdate the intrusion of an ~650 m thick dolerite sill. Deeper structures are less well resolved, although steep events and vergence folds indicate the basement is a series of thrusts (Figure 10).

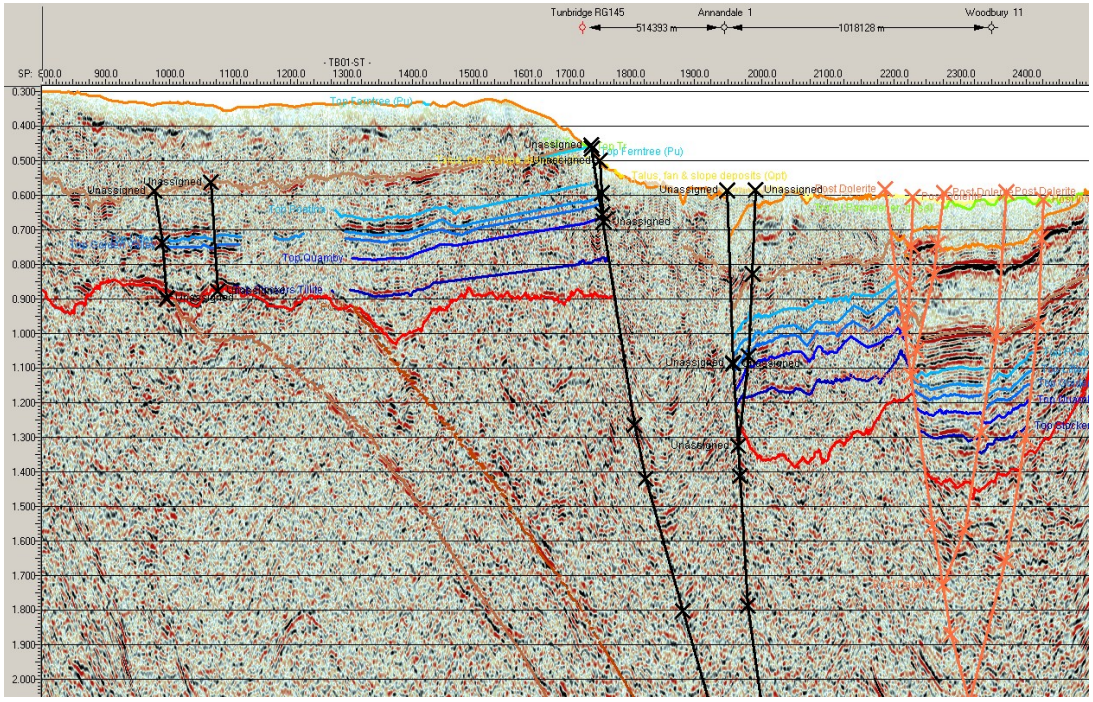

Figure 10: Interpretation of the eastern end of seismic line TB-01 ST.

Conclusions

The variable quality of the seismic data, plus the design and spacing of the survey make reliable interpretation of the seismic over the area extremely difficult and the production of realistic Two Way Time or Depth Structure maps is therefore not a real possibility. The seismic data, despite its limitations indicates that:

1. The sedimentary units that comprise the Tasmania Basin are horizontal to sub-horizontal,

2. No growth faults are recognised in the seismic data, indicating that much of the structuring probably took place after sedimentation had ceased. The basin has variously been labelled a sag basin (Veevers 1984), and a foreland basin(Collinson et al. 1987), however sedimentation rates are an order of magnitude slower than classic foreland basins (Schwab 1986). The history of sedimentary accumulation is more typical of a continental margin ("pericratonic") basin (Stacey & Berry in press). Interpretation based on isopach maps have led to the conclusion that the Tasmania Basin developed on a glacially modified landscape with about 1 km of relief, with a depocentre about the Tamar Fracture System which appeared to sink more rapidly (Banks 1989). The data could also be interpreted as the result of growth on a west dipping normal fault (Fig 11). Further evidence or structural control is seen in north and northwestern Tasmania. The boundary between the Devonport-Port Sorell Sub-basin and the Forth Metamorphics (Everard et al. 1996) is an east dipping normal fault, although this fault could be younger than the basin. While approximately 300 m of normal growth is evident on an east dipping fault adjacent to the Arthur Lineament (Burns 1963), suggesting reactivation of the Arthur Lineament during the Late Carboniferous to Early Permian.
3. The lack of major faults across the Central Highlands suggest the highlands acted as a competent block during uplift and erosion in the mid-late Cretaceous, with faulting focused along the north and east of the block. While major movement is interpreted along the Tiers and Castle Carey faults, that bound the Tertiary basins in the north of the state.
4. On the basis of the seismic data, two possible trap geometries should be considered:
    i. Across the Central Highlands where there is scant indication of large scale fault movement, traps would probably be formed by low amplitude anticlines, possibly the result of dolerite intrusion or by Mio-Pliocene NNW compression, however there is very little evidence of neotectonic structures in Tasmania.

ii. Off the highlands, traps are likely to be formed in fault blocks resulting from Tertiary movement (Fig 10).

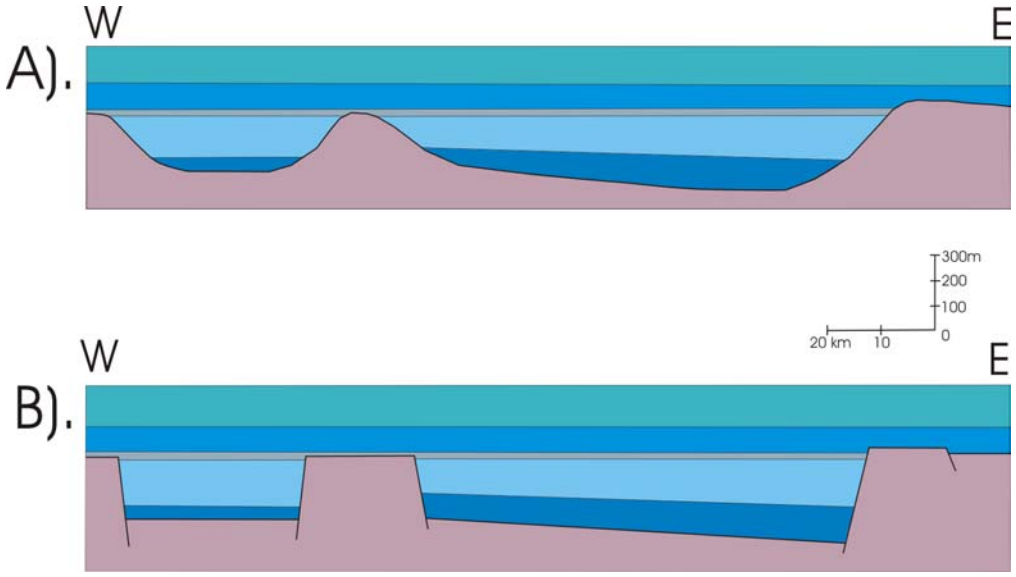

Figure 11: Two models for the initial development of the Tasmania Basin: A). Infilling of glacial valleys, B). Growth on a west-dipping fault.

Assessment of high resolution DEM

Major structuring related to the break up of Gondwanaland and the opening of the Tasman Sea ceased by the end of the Eocene. The vertical displacement of the Early Tertiary faults can still be recognised in the modern topography. A new high-resolution digital elevation model (DEM) for Tasmania (DPIWE 2002) (Figure 12) has greatly simplified the recognition of these structures.

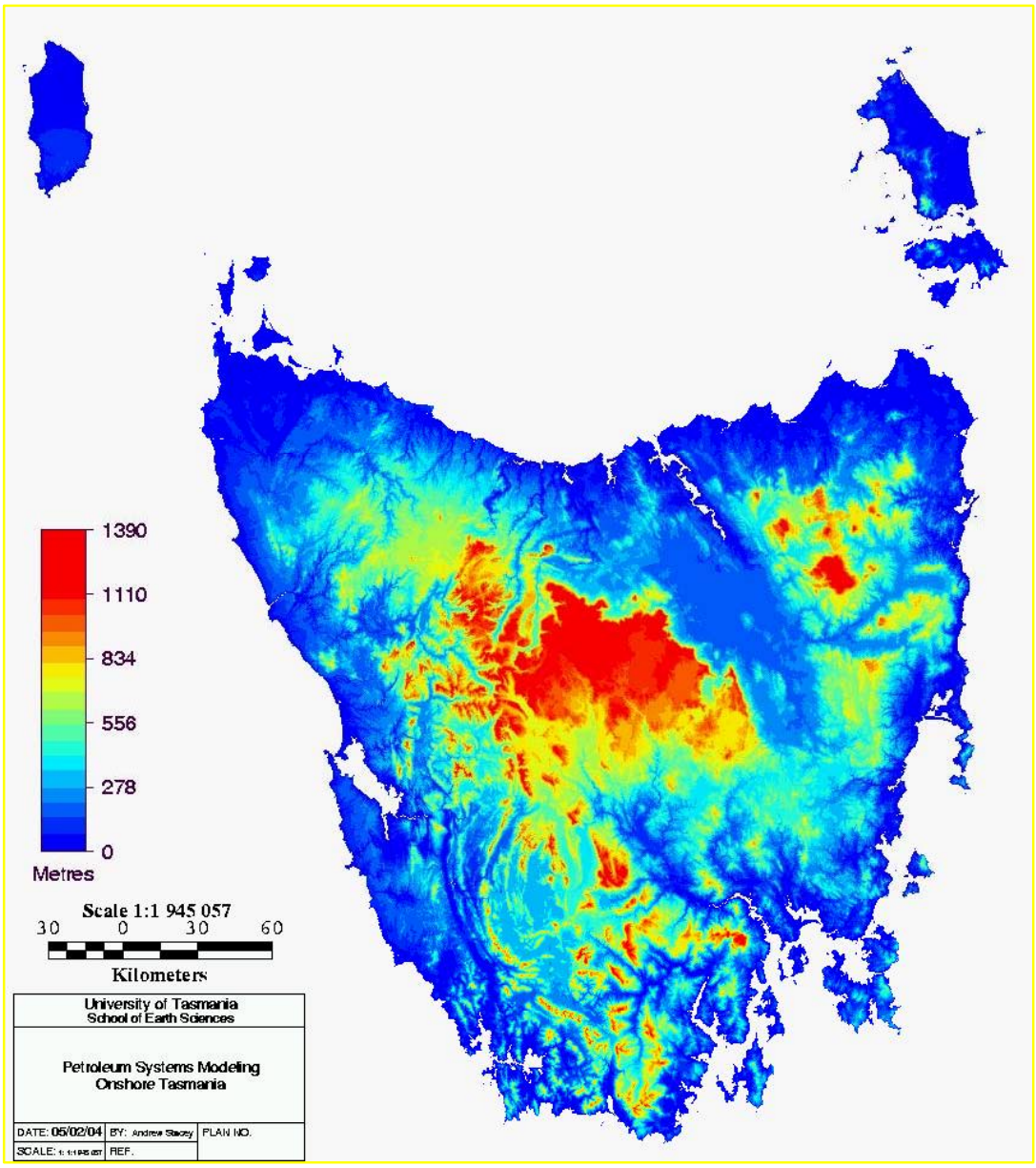

Figure 12: High resolution (25 m) Digital Elevation Model (DEM) of Tasmania (DIPWE 2002)

Aim

The aim of this study is to combine assessments of a high resolution DEM, extant geological and geophysical mapping, fission track data, fault striation data and other data sets to generate maps of fault patterns and orientations of palaeo-surfaces. These data can be used to interpret a history of fault formation and reactivation, which can be used as a tool to interpret the geometries and timing of structures that have affected the Tasmania Basin. These results can then be used to interpret migration paths and zones where traps may have formed, providing a focus for future exploration.

This work is still in progress, and thus far a DEM representing an interpretation of a mid-Tertiary surface has been produced.

Methodology

Lineament Analysis

A lineament analysis was the initial step in this study; the analysis was performed at a number of scales with simulated illumination from 2 directions 90 degrees apart (Fig 13). The main aim of this analysis was to highlight major linear features that may be associated with structures; it was also a useful vehicle for viewing the overall geometry and complexity of various features zones within the study area. From figure 13 a NW trend in the north and south are observed, while in the central and east of the area a more N-S, E-W trend is seen.

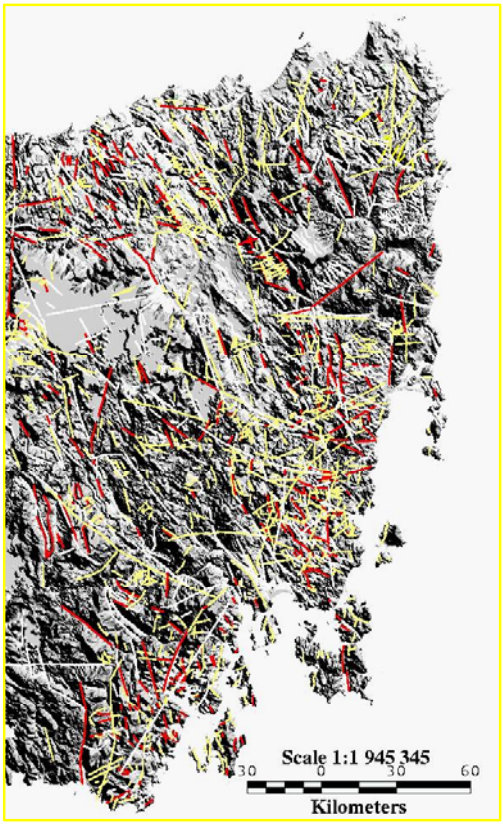

Figure 13: Composite lineament map, lineaments detected with a NE sun-angle in white, and those from the SE are in yellow, while lineaments in red were detected from both directions.

Topographic Breaks

The tectonic history of Tasmania suggests that most of the components of the present landscape are the result from structuring related to the breakup of Gondwana, which ceased by the Eocene. The vertical displacement resulting from these tectonic events can still be recognised in the modern topography.

Figure 12 shows the high and low relief surfaces. The major breaks in topography observed are the boundaries of the Tamar Graben, Devonport-Port Sorell and Longford Sub-basins and, the valleys formed by the South Esk and St Paul's Rivers. Further south breaks are evident

along the southwestern boundaries of the Upper and Lower Derwent Grabens, along the southeastern edge of the Hartz Range, and also along the Northeastern edge of Bruny Island and the Tinderbox Hills.

Tertiary fault pattern

The topographic breaks were combined with the results of the lineament analysis to generate an interpretation of Tertiary fault patterns. Figure 14 shows the resultant Tertiary fault pattern draped over the DEM. The identifiable pattern is a series of northwest trending structures in the south, a complex transfer zone to their north and east and another series of northwest structures in the north.

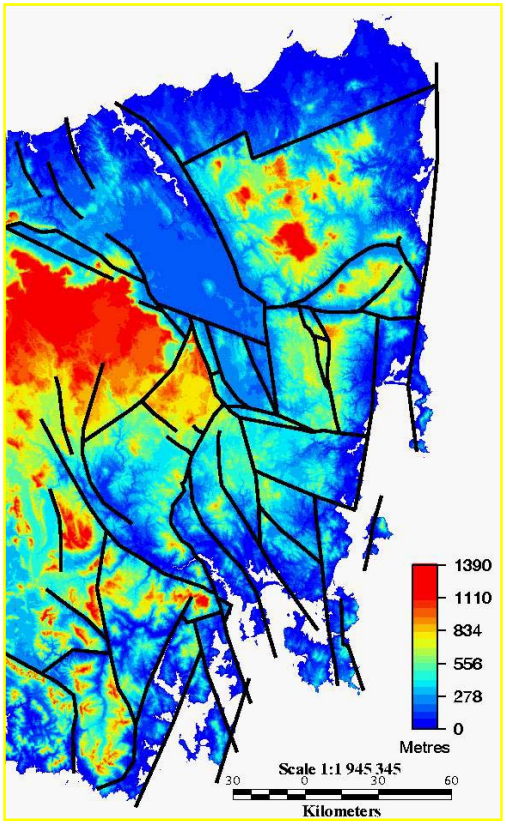

Figure 14: Tertiary fault pattern interpreted from the DEM.

In the north, the large-scale topographic depressions produced by the Tamar Graben, the Devonport-Port Sorell and the Longford Sub-basins, are easily observed on the DEM, as are the main boundary faults of these structures (Fig 15). The most obvious is the Tiers Fault, a major structure with several hundreds of metres of normal movement in the Early Tertiary. Erosion was greatest in the NE with only remnants of Permian strata remaining on dolerite-capped hills, indicating that uplift and subsequent erosion was probably at its greatest in this area (Fig 16).

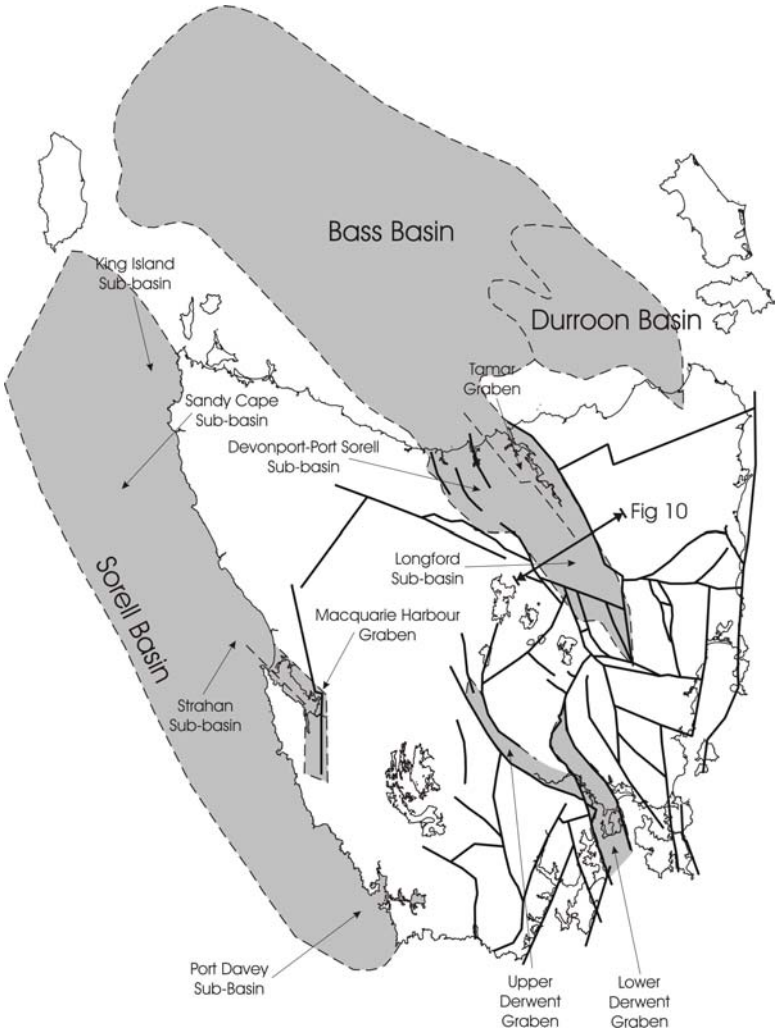

Figure 15: Late Jurassic to Middle Tertiary structures and fault patterns interpreted from the high resolution DEM.

Figure 16: 1:250 000 Geology draped over the DEM. Note: nearly all the Permian strata has been removed in the northeast of Tasmania.

In the Devonport-Port Sorell Sub-basin analysis of the DEM shows three NNW striking faults including the east and west boundary of the basin, while the southern boundary is the uplifted Central Plateau (Fig 15).

In the south, analysis of the DEM shows the Derwent Graben actually consists of two linked structures, the lower and upper Derwent Graben. The Lower Derwent Graben is a narrow NW trending structure, bounded on the west by the Cascades Fault system and by the Meehan Ranges in the east. The structure contains only a few hundred metres of sediment, the oldest

being of Paleocene age, indicating faulting initiated in the early Tertiary (Colhoun 1989). Analysis of the DEM indicates the structure is paralleled by the Derwent Valley as far north as Bridgewater where it continues NW followed by the course of the Jordan River, and terminating near Melton Mowbray. The throw on the Cascades system decreases to the north from Hobart.

The Upper Derwent Graben is bounded on its southwestern side by a shallowly concave normal fault, down to the NE that approaches the Cascades Fault near Hobart. The fault follows the upper Derwent Valley before dying out in a horsetail splay on the Central Plateau. The intersection between the two faults is a lateral ramp, with no direct connection between the two structures. Curved, non-linked faults as identified here are indicative of a regime of low extension, while the overall complexity of the observed pattern may indicate oblique extension (McClay et al. 2002), although an element of inheritance cannot be discounted.

Palaeo surface identification

The final step in the production of the Tertiary DEM is to identify the orientation of the Palaeo-surface in each of the fault bounded blocks from the relict topography. In some blocks interpreting the orientation of the palaeo-surface is reasonably straightforward. For example in the large northeastern block there remains numerous relict high to constrain the geometry of the interpreted surface. However, in areas that have been highly eroded, like the area to the NW of Hobart, interpreting the geometry of the surface from the relict topography becomes far more subjective, and in this case clues such as the course of major drainage systems are used to advance the interpretation.

Once the orientation of the surface has been identified, several points are selected from within each block. The points are grided using Surfer 7™ software, using a minimum curvature algorithm, a 1000 m grid and griding using a function that grids around the interpreted fault boundaries and not across them. The result is that for each block a surface is produced with a unique orientation based on the points chosen (Fig. 17).

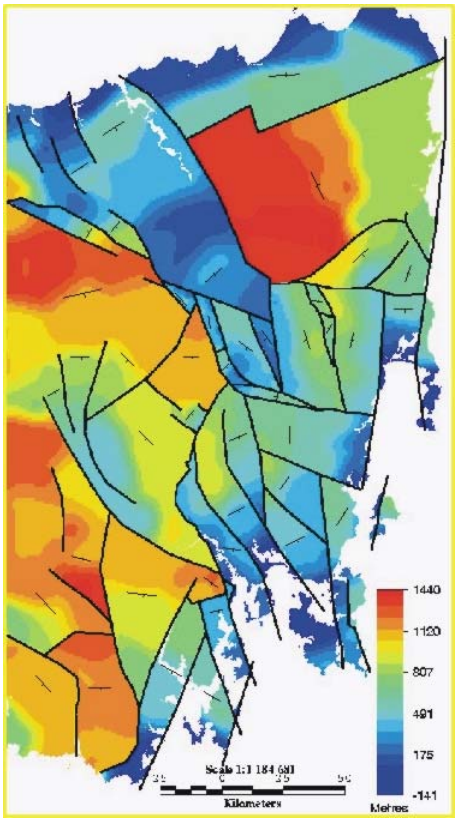

Figure 17: DEM representing the Mid-Tertiary.

Further work

Further work on the DEM will involve the generation of a DEM representing a Permian surface across the study area, probably the boundary between the Upper and Lower

Parmeener supergroups and compare that DEM with the DEM for the Tertiary surface and interpret a pattern of post-Permian faulting.

Other datasets to be integrated with the DEM's to constrain the interpretation are:

- Magnetics and gravity data to constrain the location of the interpreted faults,
- Apatite Fission Track data to identify the timing of uplift and erosion from across the study area,
- The quantity of Late Jurassic – Early Tertiary erosion in could also be estimated by subtracting the Permian DEM for that of the Tertiary, and comparing the result with estimated volumes of Jurassic-Cretaceous sediments deposited in the offshore basins, which would also constrain the model.

By synthesising all these elements predict the effect that the post Permian and Tertiary structural development has had on the migration of hydrocarbons, which forms the main conclusion to the research and thesis.

References

BANKS, M. R., 1989, Late Carboniferous - Triassic: Summary and structural development. In: Burrett, C. F. and Martin, E. L. (Eds.), Geology and mineral resources of Tasmania, Geological Society of Australia, Special Publication 15, 293-294.

BURNS, K. L., 1963, Trowutta Geological Atlas 1 mile Series N8115 & IV (zone 7 sheet 29), Tasmania Department of Mines.

COLHOUN, E. A., 1989, Cainozoic Geomorphology. In: Burrett, C. F. and Martin, E. L. (Eds.), Geology and mineral resources of Tasmania, Geology Society of Australia, Special Publication 15, 403-409.

COLLINSON, J. W., KEMP, N. R. AND EGGERT, T. J., 1987, Comparison of Triassic Gondwana sequences in the Transantarctic mountains and Tasmania. In: McKenzie, G. D. (Eds.), Gondwana Six: Stratigraphy, sedimentology and paleontology, Geophysical Monograph, 51-61.

DPIWE, 2002, 25m Digital Elevation Model (DEM), derived from 1:25 000 scale mapping Department of Primary Industries, Water and Environment, Tasmania.
EVERARD, J. L., SEYMOUR, D. B. AND BROWN, A. V., 1996, Devonport Geological Atlas 1:50000 series, sheet 7915N, Tasmanian Geological Survey.
FAIRBRIDGE, R. W., 1949, Geology of the Country around Waddamana, Central Tasmania. Papers and Proceedings of the Royal Society, Tasmania, 1948., 111-147.
FOURNIER, P., 2000, The design of a Sonde used to measure Seismic Velocities and Temperature, Tasmania Basin. Honours (unpublished), School of Earth Sciences, University of Tasmania, Hobart.
LANE, P., 2002, Seismic Interpretation and Basin Analysis of the Longford Sub-Basin. B.Sc Honours Thesis (unpublished), School of Earth Sciences, University of Tasmania, Hobart.
MCCLAY, K. R., DOOLEY, T., WHITEHOUSE, P. AND MILLS, M., 2002, 4-D evolution of rift systems: Insights from scaled physical models. AAPG Bulletin, 86, 6, 935-959.
SCHWAB, F. L., 1986, Sedimentary 'signitures' of foreland basin assemblages: real or counterfeit? In: Homewood, P. (Eds.), Foreland Basins, International Association of Sedimentologists, Special Publication 8, 395-410.
STACEY, A. R. AND BERRY, R. F., in press, The structural history of Tasmania, a review for petroleum explorers. Eastern Australian Basin Symposium 2.
TANNER, D. AND BURRETT, C., 1997, 1997 Annual Exploration Report. Unpublished Report, Great Southland Minerals,
TEARPOCK, D. J. AND BISCHE, R. E., 2003, Applied Subsurface Geological Mapping with Structural Methods, Prentice Hall, Upper Saddle River, New Jersey.
VEEVERS, J. J. (Ed.) 1984, Phanerozoic earth history of Australia, Clarendon Press, Oxford,
WILLIAMS, E., MCCLENAGHAN, M. P. AND COLLINS, P. L. F., 1989, Mid-Palaeozoic Deformation, Granitoids and Ore Deposits. In: Burrett, C. L. and Martin, E. L. (Eds.), Geology and Mineral Resources of Tasmania, Geological Society of Australia, Special Publication 15, 238-291.
WU, J., 1996, Potential pitfalls of crooked-line seismic reflection surveys. Geophysics, 61, 1, 277-281.